SPACE SCIENCES

Nature, formation, and distribution of carbonates on Ceres

Filippo Giacomo Carrozzo,[1]* Maria Cristina De Sanctis,[1] Andrea Raponi,[1] Eleonora Ammannito,[2] Julie Castillo-Rogez,[3] Bethany L. Ehlmann,[3,4] Simone Marchi,[1,5] Nathaniel Stein,[4] Mauro Ciarniello,[1] Federico Tosi,[1] Fabrizio Capaccioni,[1] Maria Teresa Capria,[1] Sergio Fonte,[1] Michelangelo Formisano,[1] Alessandro Frigeri,[1] Marco Giardino,[1] Andrea Longobardo,[1] Gianfranco Magni,[1] Ernesto Palomba,[1] Francesca Zambon,[1] Carol A. Raymond,[3] Christopher T. Russell[6]

Different carbonates have been detected on Ceres, and their abundance and spatial distribution have been mapped using a visible and infrared mapping spectrometer (VIR), the Dawn imaging spectrometer. Carbonates are abundant and ubiquitous across the surface, but variations in the strength and position of infrared spectral absorptions indicate variations in the composition and amount of these minerals. Mg-Ca carbonates are detected all over the surface, but localized areas show Na carbonates, such as natrite (Na_2CO_3) and hydrated Na carbonates (for example, $Na_2CO_3{\cdot}H_2O$). Their geological settings and accessory NH_4-bearing phases suggest the upwelling, excavation, and exposure of salts formed from Na-CO_3-NH_4-Cl brine solutions at multiple locations across the planet. The presence of the hydrated carbonates indicates that their formation/exposure on Ceres' surface is geologically recent and dehydration to the anhydrous form (Na_2CO_3) is ongoing, implying a still-evolving body.

INTRODUCTION

Carbonates are components of chondritic meteorites [for example, (*1*, *2*)] and have typically been used to infer the occurrence of liquid water in their parent bodies (*3*). The carbonate signature in Ceres' spectrum (3.3 to 4.0 μm) was first detected on Earth (*4*, *5*) and then confirmed by Dawn observations showing that Ceres' average surface is an assemblage of Mg phyllosilicates, ammoniated species, dark materials, and Mg-Ca carbonates (*6*). The carbonate absorption in the Ceres spectrum is deeper than in so-far measured spectra of carbonaceous chondrites (CC), suggesting a larger abundance of carbonates on Ceres than in typical CC (*7*).

Ceres' overall composition and the ubiquitous distribution of the OH- and NH_4-bearing species indicate a pervasive, past aqueous alteration involving ammoniated fluids and Mg phyllosilicate formation (*8*). The discovery of abundant carbonate as the main constituent of the bright material in Occator crater (*9*) indicates a different style of aqueous alteration locally. The carbonate found in Occator, natrite (Na_2CO_3), is different from the Mg-Ca carbonate detected in the global Ceres spectrum, and it is not observed in CC (*9*, *10*). The distribution and chemical composition of the carbonates are thus tracers of complex and varying aqueous chemical processes on Ceres.

Carbonates exhibit diagnostic absorption features due to vibrational energy level transitions of the CO_3^{2-} group. The fundamental modes correspond to wavelengths of ~7, ~11.5, and ~14 μm, but strong overtone and combination bands occur at ~3.3 to 3.5 μm and ~3.9 to 4.0 μm (*11*). A visible and infrared mapping spectrometer (VIR) (*12*) on board the Dawn spacecraft mission operates between 0.25 and 5.1 μm, encompassing several carbonate absorptions, such as the strong ~3.3- to 3.5-μm and ~3.9- to 4.0-μm features. We measured the strength and position of the ~3.9-μm feature across Ceres (Fig. 1; see also the Supplementary Materials) that gives us the distribution of carbonates unambiguously. The band at 3.3 to 3.5 μm is not mapped because this spectral region has contributions from overlapping absorptions of ammoniated phyllosilicates, carbonates, and organic compounds. All these materials have been detected on Ceres (*4*, *8*, *9*, *13*), and disentangling the contributions of different components in the 3.3- to 3.5-μm spectral region is extremely challenging.

Spectral analysis and carbonate distribution

The maps (Fig. 1) have global longitudinal coverage, latitudinal coverage from 66°S to 66°N, and a spatial resolution of ~1.86 km per pixel at the equator. A few selected small areas, discussed afterward, have also been observed at higher resolution, at ~100 m per pixel. The map shows that the carbonate band position is mostly uniform across the surface (average band center at 3.947 ± 0.005 μm), indicative of Mg or Mg-Ca carbonates {for example, magnesite ($MgCO_3$) or dolomite [$MgCa(CO_3)_2$]}, with the exception of a few recognizable kilometer-size areas displaying band centers at longer wavelengths, up to 4.02 μm, consistent with natrite (Na_2CO_3). The map of carbonate band strength (Fig. 1B) shows similar values across most of the surface (0.063 ± 0.004), but several localized kilometer-size areas exhibit bands of larger intensity relative to the background. Representative spectra of areas showing different values of band centers and intensity are displayed in Fig. 2.

The band center map shows some regions with intermediate values that could suggest the presence of other types of carbonates or a mixture of Mg-Ca and Na carbonates. To distinguish between these two hypotheses, we fit a spectrum representative of these intermediate regions with different types of carbonates (that is, $CaCO_3$, $MnCO_3$, and $FeCO_3$) and with a mixture of Mg-Ca and natrite (fig. S5). A mixture of dolomite and natrite gives an excellent fit, but Mn carbonate (for example, rhodochrosite) and Ca carbonate (for example, calcite) also give good fits. However, the occurrence of most of these areas with intermediate band center values adjacent to areas rich in Na carbonates and Mg-Ca carbonates suggests a mixture of Mg-Ca and Na carbonates (Fig. 3). Moreover, when these broad areas are observed at higher spatial resolution, the intermediate values are often resolved into smaller areas with a band center at ~4 μm, compatible with Na carbonates, and at ~3.96 μm.

[1]Istituto di Astrofisica e Planetologia Spaziali, Via del Fosso del Cavaliere 100, 00133 Roma, Italy. [2]Agenzia Spaziale Italiana, Via del Politecnico, 00133 Roma, Italy. [3]Jet Propulsion Laboratory, California Institute of Technology, Pasadena, CA 91109, USA. [4]Division of Geological and Planetary Sciences, California Institute of Technology, Pasadena, CA 91125, USA. [5]Southwest Research Institute, 1050 Walnut Street, Boulder, CO 80302, USA. [6]Earth Planetary and Space Sciences, University of California, Los Angeles, CA 90095, USA.
*Corresponding author. Email: giacomo.carrozzo@iaps.inaf.it

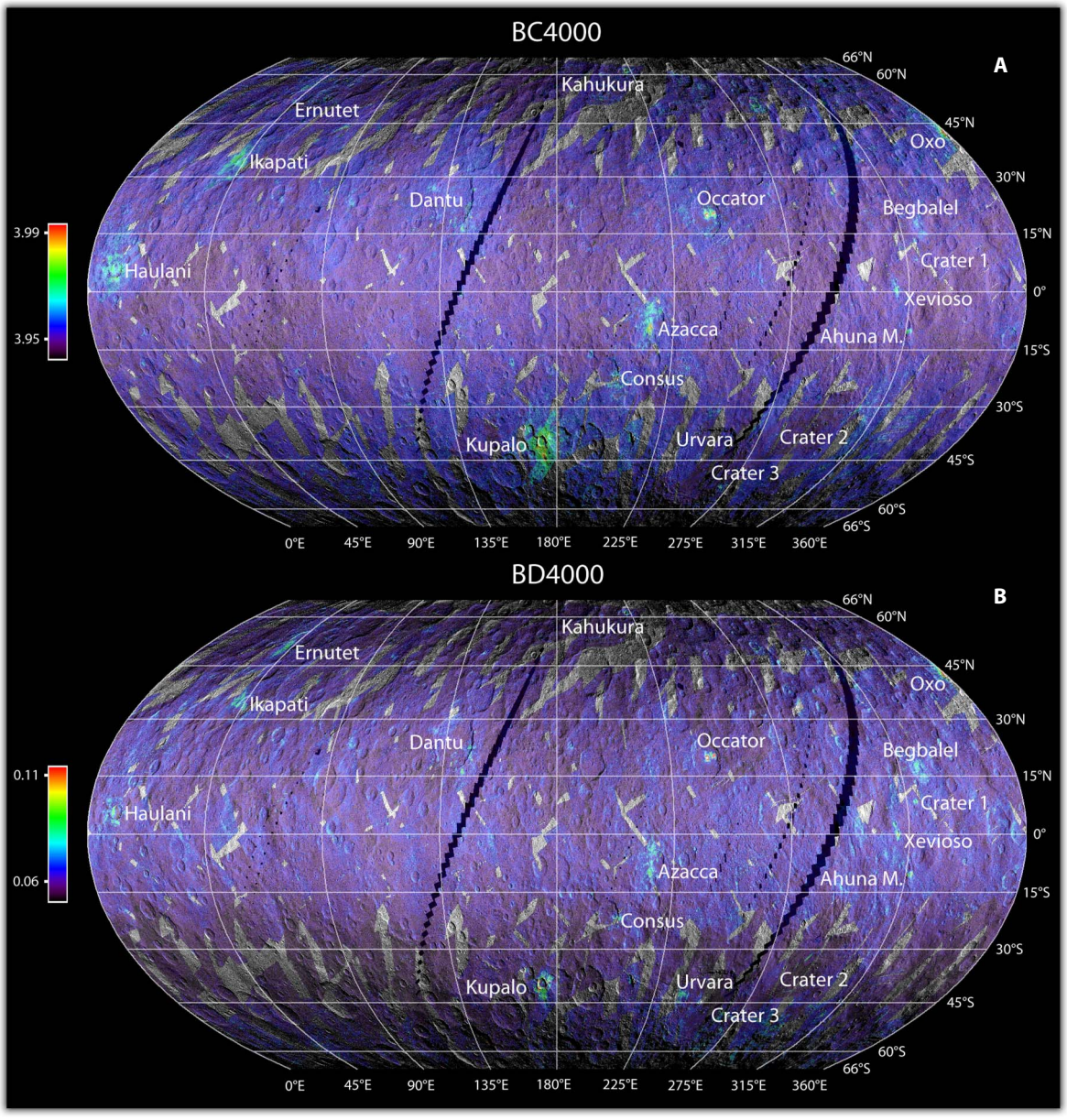

Fig. 1. Distribution and intensity of the carbonate absorption in VIR data. (**A**) Central wavelength and (**B**) intensities of the 3.9-μm absorption feature. The maps are superimposed on the Framing Camera images using a transparency of 25%.

From the global maps, we conclude that carbonates are present on the whole observed surface of Ceres (Fig. 1), and the spectra of most of the terrains are consistent with Mg-Ca carbonates. A few areas stand out from the global distribution, particularly bright spots near impact craters (*14*) and Ahuna Mons (*15*). Notably, Oxo (42°N, 359°E), Occator (20°N, 240°E), Azacca (6°S, 218°E), Kupalo (39°S, 173°E), Ikapati (33°N, 46°E), and Ahuna Mons (10°S, 317°E) are the most representative regions where carbonate exhibits the highest intensity, with absorptions centered between 3.98 and 4.02 μm (Figs. 1 and 3, and figs. S1 and S3).

We observe that most of the regions with strong absorptions have band centers at longer wavelengths (Fig. 4). However, a few exceptions are recognizable: Ernutet crater, Urvara crater (western side), and some small areas in Baltay Catena. The region around Ernutet crater, where organic-rich material has been discovered (*13*), also stands out in the band depth map. In this region, only a few small areas show band centers at slightly longer wavelengths (~3.96 μm), whereas most of the region has band centers similar to the average Ceres values (fig. S1) (*13*). The western side of the Urvara crater (fig. S2) and the region extending from ~48°S, 260°E to ~49°S, 280°E (near Baltay Catena; fig. S2) are also characterized by small localized areas with stronger absorption bands without a shift of the band wavelength (see arrows in fig. S2B). Spectral modeling of these areas indicates that best fit is obtained using dolomite (fig. S4).

Most of the areas showing enhanced band depths and centers at longer wavelengths broadly match areas showing fainter phyllosilicate band depths (*9*, *14*). Assuming that band depths are primarily indicators of

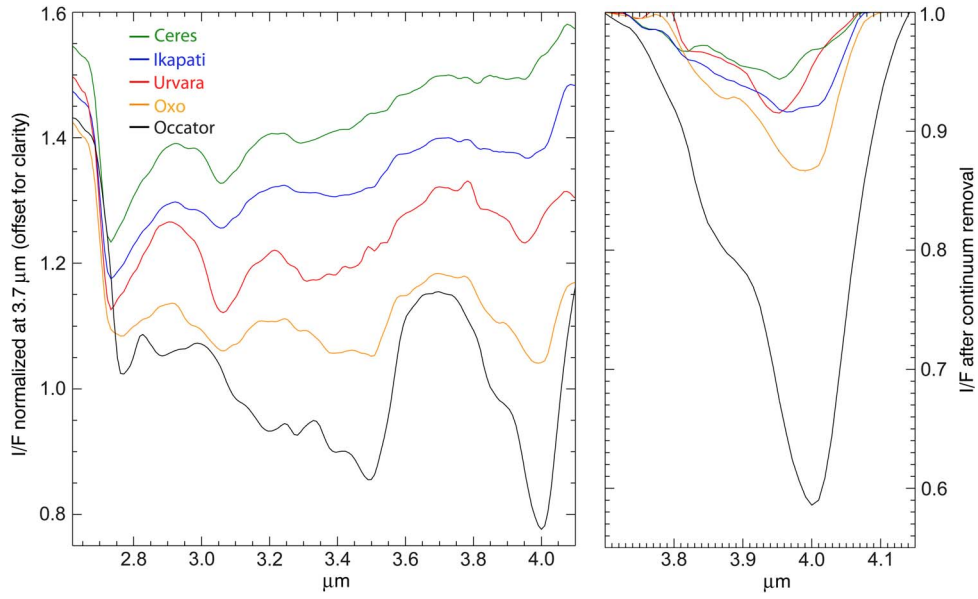

Fig. 2. Average VIR spectrum of Ceres and VIR spectra from different areas enriched in carbonates. Left: The spectra have been normalized to 1 at 3.7 µm and offset for clarity. **Right:** Continuum-removed spectra between 3.7 and 4.2 µm show the shift in central wavelength of the 3.9- to 4.0-µm carbonate band. The spectra (average of eight pixels) are taken at resolution of ~1.86 km per pixel. I/F is a reflectance factor.

the amount of the mineralogical species responsible for the absorptions, the anticorrelation between phyllosilicate and carbonate intensities suggests an inverted proportion between the two components.

Looking at the high-resolution spectra (~100 m per pixel), we discover that although most of the carbonate-rich areas (Fig. 1) are consistent with the presence of Na_2CO_3, some small areas in specific locations, such as in Oxo (Fig. 5), Azacca, Kupalo, and Kahukura, are different and cannot be fully fit using Na_2CO_3 (table S2). The spectra of these small areas, typically extending from 0.01 to a few square kilometers, show an overall blue spectral slope across the 1.0- to 4.2-µm range, indicative of changes in the composition and/or physical properties of the materials (*16*), and a larger and broader band in the 2.6- to 3.8-µm range, suggesting hydration. Different species can account for the hydration features as shown by spectral fits performed with different hydrated species (Fig. 5 and fig. S6). The results indicate that the species with the highest number of water molecules trialed, that is, natron ($Na_2CO_3{\cdot}10H_2O$), cannot fit the spectra, whereas species with less water give excellent fits. The best fits are obtained using thermonatrite ($Na_2CO_3{\cdot}H_2O$; see Fig. 5) or trona ($NaHCO_3{\cdot}Na_2CO_3{\cdot}2H_2O$; see fig. S6), but good fits are also obtained with other hydrated sodium carbonates. Pixel-size areas rich in hydrated sodium carbonate are mainly recognized in the high-resolution data (~100 m per pixel), close to areas with Na carbonate, implying that the areal extent of these species is small and discrete, and consideration of spatial mixing effects is important for their identification. Thus, there may be more areas exposing hydrated sodium carbonate, and most of the region where we identify Na_2CO_3 could be actually mixtures containing also the hydrated forms.

Hydrated sodium carbonates occur in different morphological settings. In some places, such as Oxo crater and Kahukura crater (*17*), Na_2CO_3 and its hydrated forms are found in the same area where H_2O ice has been detected (fig. S3) (*18*). Hydrated sodium carbonates are also found in areas devoid of ice, such as Kupalo crater (*19*). Thus, the association between hydrated sodium carbonate and water ice is not consistently associated with the presence of water ice.

RESULTS AND DISCUSSION

A pre-Dawn scenario suggested that Ceres' surface carbonates may have formed in part through impact-facilitated oxidation of organic matter (*20*). Other models suggest that Mg-Ca carbonate formed with the rock as part of a global hydrothermal event, when Ceres was altered from the original anhydrous mineralogy by aqueous fluids, following accretion, because of ^{26}Al decay heat (*21*). Another suggests formation from a second-generation aqueous episode by oxidation of organic matter via reaction with sulfates (*22*). The presence of Na and Mg-Ca carbonates indicates that the liquid was relatively alkaline and should have contained a large fraction of chlorides and alkali/alkaline elements, as has been predicted for fluids reacting with chondritic material at low water/rock (*23*).

The local and recent exposure of anhydrous and hydrated Na carbonates may indicate separate processes (*23*, *24*). If Ceres originated from a material typical of the outer solar system (*6*), it would contain abundant ices of $CO_2/CO/NH_3$. Thus, fluids would be similar in composition to the Na-NH_4-Cl-CO_3–rich fluids in some satellites of the outer solar system (*24*–*26*). Hydrated Na carbonates could form early in a global ocean in equilibrium with the altered rocky phase and be incorporated in Ceres' crust upon freezing of that ocean (*21*). The source and timing of the mobilization of sodium carbonate–rich fluids remain an open question. Different mechanisms can be invoked: (i) local formation via impact-induced heating in the presence of ice (*9*, *22*, *27*, *28*) and (ii) aqueous upwelling from depth via fractures (*29*) or conduits of Na carbonates present in residual brines if Ceres' deep interior temperatures are favorable (*9*, *28*). Both scenarios assume the existence of relatively modern brines of various salts, for example, chlorides, NaCl, and NH_4Cl (*9*, *22*, *28*) mixed with ice and possibly silicates and clathrates (*27*, *30*), including natron ($Na_2CO_3{\cdot}10H_2O$), trona ($NaHCO_3{\cdot}Na_2CO_3{\cdot}2\ H_2O$), and/or $NaHCO_3$ depending on the freezing conditions of Ceres' early ocean (*9*, *26*, *27*, *31*). Quasi-uniform distribution of Mg-Ca carbonates across the surface suggests a pervasive alteration process to deposit these low-solubility phases.

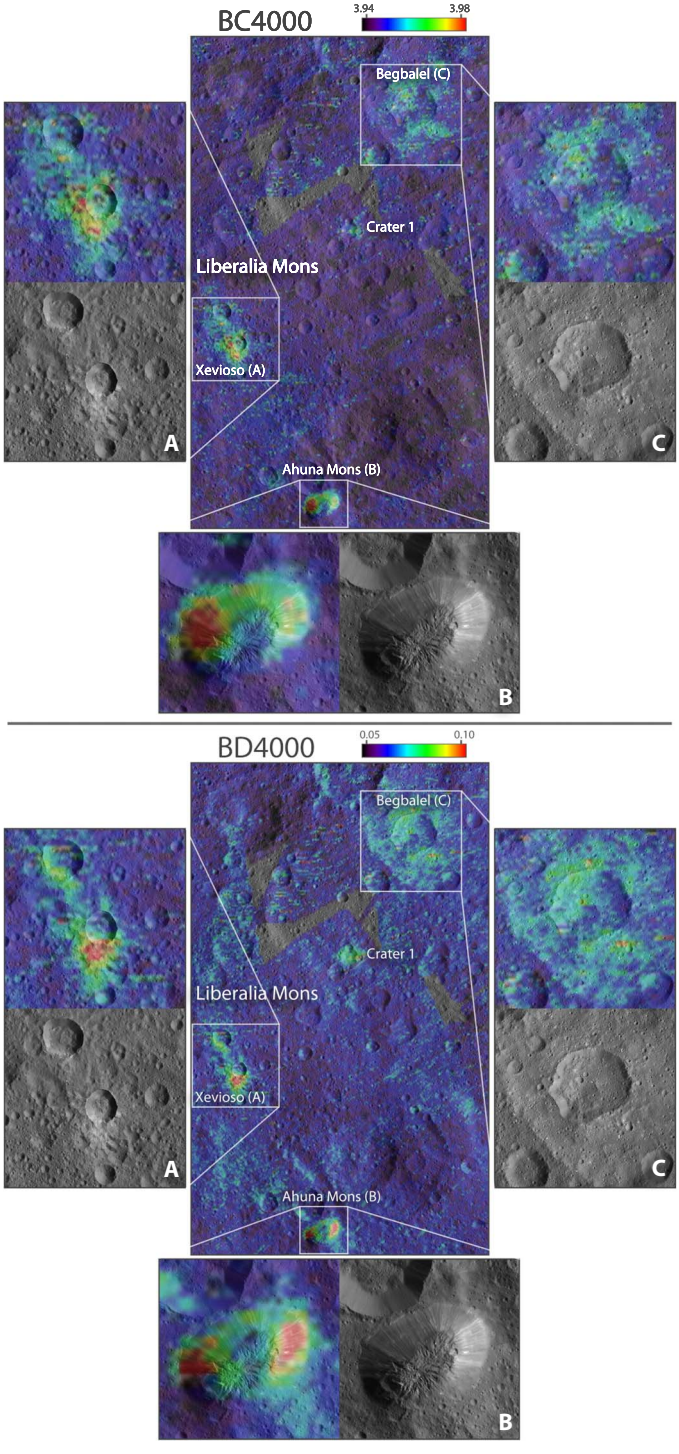

Fig. 3. Distribution of carbonate band center and band depth in a region close to Ahuna Mons and Liberalia Mons. Zoom on (**A**) Xevioso crater, (**B**) Ahuna Mons, and (**C**) Begbalel.

In scenario 1, local formation via impact heating leads to the melting of ice and aqueous solutions containing different ions, including abundant Na^+, Cl^-, CO_3^{2-}, NH_4^+, and HCO_3^-. Freezing and/or evaporation leads to the precipitation of corresponding salts; models and laboratory experiments show that hydrated Na carbonates of varying hydration states are the first and most abundant precipitates (*26*, *27*). Ammonium carbonates and/or chlorides are detected (*9*) and could be formed from NH_4^+ released from the clays. They are one of the last precipitates (along with spectrally less-detectable NaCl), only form from specific fluid chemistries, and are phases predicted to be unstable at Ceres' surface (*26*, *27*). Fluid variation could explain the heterogeneity of the observed distribution as the result of local creation of Na carbonates and NH_4 salts by impacts or their upwelling at impact sites (*22*, *28*).

Scenario 2 is based on previous and recent global thermal evolution models (*21*, *32*), and inference from the modeling of Ahuna Mons (*33*) that involves ascent of cryo-magma and extrusion onto the surface from a reservoir at depth, as well as topography relaxation (*31*), indicating that brines may be present at several tens of kilometer depth. This is due to the combination of Ceres' relatively warm surface and the depression of the eutectic temperature by the presence of salts, by as much as ~30° (*27*). The extrusion mechanism could involve stressing of the brine reservoir [for example, via compression (*33*)], gas-driven buoyancy (*34*), and even access via large fractures opened by impacts (*29*).

Some occurrences of Na_2CO_3 are related to recently upwelled material from the subsurface, such as Occator's central dome and Ahuna Mons (*9*, *15*). In other cases, sodium carbonate is found in crater ejecta and floors, such as Kupalo and Haulani, or in small bright exposures, such as in Ikapati crater. Most of the places with Na carbonates are associated with or close to domes and mounds, such as those close to or inside Haulani, Oxo, Dantu, and Azacca and the areas within Ahuna Mons and Liberalia Mons (Fig. 3), although not exactly superimposed. Moreover, craters such as Haulani and Ikapati also have morphologies, such as floor fractures, that may be indicative of upwelling processes.

The correlation of Na carbonates with some extrusive constructs suggests that at least some Na carbonates are transported to, or near to, the surface by ascending subsurface fluids in several areas of Ceres. However, the association of Na carbonate with young craters could be consistent with the material mobilized or created by impact-induced heating. The data are not sufficient to fully discriminate among the possible mechanisms, and likely, the types of Na carbonates and the observed distribution are the results of a combination of different processes.

Nevertheless, the detection of Na_2CO_3, NH_4 salts (*9*), and hydrated sodium carbonates provides major constraints on Ceres' chemical evolution. NH_4 salts are speculated to be unstable over geologic time (*27*). Hydrated sodium carbonates are not stable on airless surfaces and dehydrate upon exposure to vacuum and irradiation over Myr timescales (*25*). Destabilization on the surface involves both dehydration and decarbonation; for example, $Na_2CO_3{\cdot}H_2O$ in $Na_2CO_3 + H_2O(g)$ (*9*, *25*, *27*). The detection of hydrated Na carbonates supports an aqueous origin of Na carbonates followed by their partial decomposition (mainly dehydration) in surface environments. This implies that sites rich in hydrated carbonates have been formed/exposed recently (a few million years), and dehydration of hydrated Na carbonates is still ongoing. This is in accordance with crater counting and modeling that predict recent formation, within tens to hundreds of millions of years (*28*, *35*).

The different chemical forms of the sodium carbonate, their fresh appearance, morphological settings, and the uneven distribution on Ceres indicate that the formation, exposure, dehydration, and destruction processes of carbonates are recurrent and continuous in

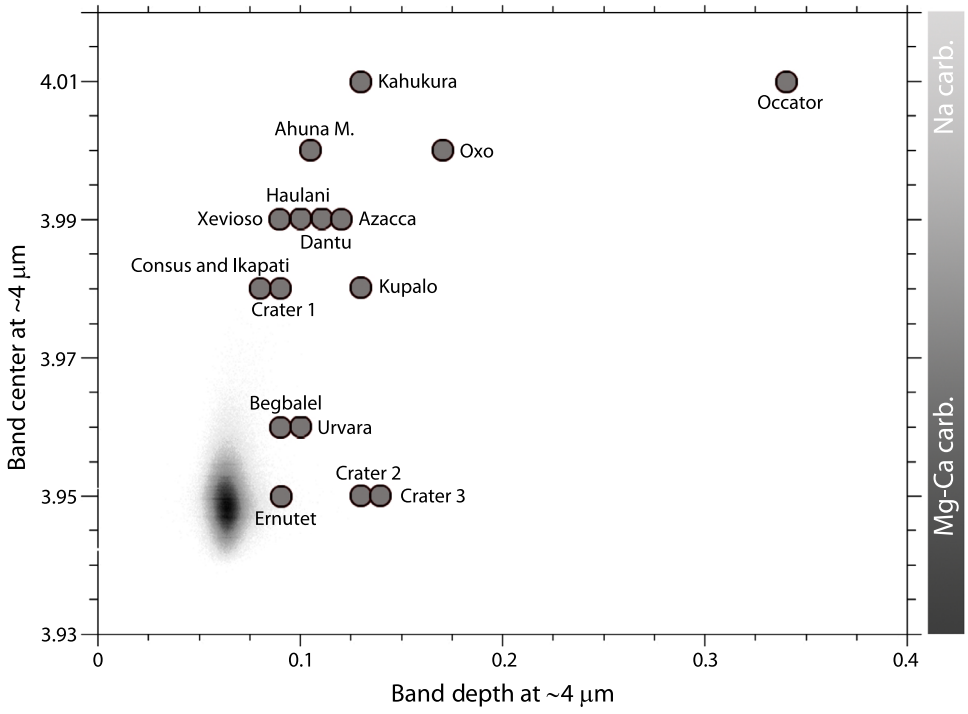

Fig. 4. Scatterplot of the band center versus band depth of the carbonate absorption. The gray bar on the right indicates the relative regions where Mg-Ca carbonates (Mg-Ca carb.) and Na carbonates (Na carb.) are located. The gray cloud represents the data from the global map of Ceres' surface as in Fig. 1.

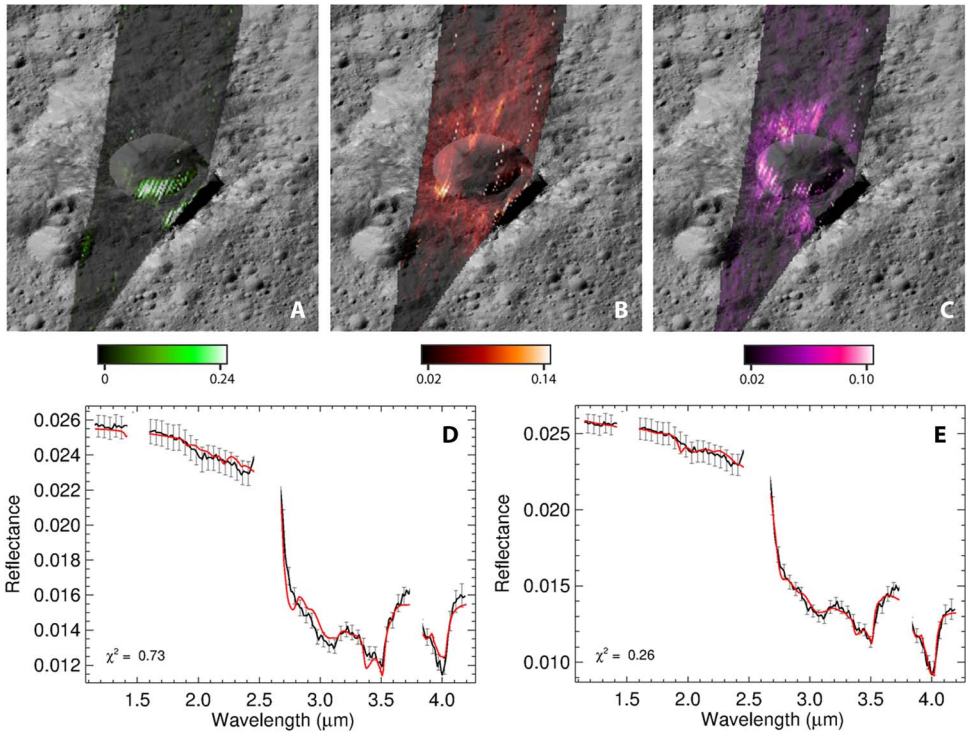

Fig. 5. Distribution of surface compounds in Oxo crater. (**A**) Water ice, (**B**) Na_2CO_3, and (**C**) hydrated sodium carbonate ($Na_2CO_3{\cdot}H_2ONa_2CO_3{\cdot}H_2O$). Mass fraction abundances are derived from the spectral fitting method (table S2). The lower panels show the spectral fit (red curve) of select pixels in Oxo using (**D**) ammonium montmorillonite, dolomite, dark material, and natrite (Na_2CO_3) excluding and (**E**) including $Na_2CO_3{\cdot}H_2O$. Error bars are calculated according to calibration uncertainties and Poisson noise (*41*).

recent geological time, implying a still-evolving body and modern processes involving fluid water.

MATERIALS AND METHODS

As in the study of De Sanctis *et al.* (*6*) and Ammannito *et al.* (*8*), we modeled the spectra as formed by an intimate mixture of different end members, starting from their optical constants. We used Hapke theory (*36*), which characterizes light scattering in particulate media. The optical constants were derived from reflectance spectra, as in the study of Carli *et al.* (*37*). The end members treated in this work are listed in table S2. The best fit between the measured spectra and the models were obtained by means of a least-squares optimization algorithm, as in the study of Raponi *et al.* (*38*), where the free parameters are as follows: (i) abundances of the end members; (ii) grain sizes of the end members; (iii) a multiplicative constant of the absolute level of reflectance of the model to account for uncertainties on the radiometric and photometric accuracy, as well as errors on the local geometry information due to unresolved shadows and roughness; (iv) a slope added to the model to better fit the measured spectrum; and (v) temperature and effective emissivity. The latter is the product of the directional emissivity (*39*), and a free parameter was used to account for unresolved shadows and the structure of the surface (*40*). Their interpretations are outside the scope of the present work.

SUPPLEMENTARY MATERIALS

Supplementary material for this article is available at http://advances.sciencemag.org/cgi/content/full/4/3/e1701645/DC1

table S1. Main regions with a high 3.9-μm band depth.

table S2. Retrieved abundances in selected pixels showing the highest concentration of carbonates in the listed areas.

fig. S1. Main regions with high 3.9-μm band depth.

fig. S2. Retrieved abundances in selected pixels showing the highest concentration of carbonates.

fig. S3. Band center and band depth maps in Ernutet and Ikapati craters.

fig. S4. Spectral fits of carbonate rich area in crater 2.

fig. S5. Spectral fits (red curve) of phyllosilicate-rich area (black curve).

fig. S6. Spectral fits (red curve) of natrite-rich area in Oxo crater (black curve, the same spectrum as in Fig. 5).

fig. S7. Spectra of the end members used in the spectral modeling.

REFERENCES AND NOTES

1. A. J. Brearley, The action of water, in *Meteorites and Early Solar System II*, D. S. Lauretta, H. Y. McSween Jr., Eds. (University of Arizona Press, 2006), pp. 587–624.
2. A. J. Brearley, R. H. Jones, Chondritic meteorites, in *Planetary Materials*, J. J. Papike, Ed. (Mineralogical Society of America, 1998), vol. 36, pp. 1–398.
3. A. J. Brearley, Meteorites and cosmochemical processes, *Treatise on Geochemistry*, A. M. Davis, Ed. (Elsevier, ed. 2, 2014), vol. 1, pp. 309–334.
4. R. E. Milliken, A. S. Rivkin, Brucite and carbonate assemblages from altered olivine-rich materials on Ceres. *Nat. Geosci.* **2**, 258–261 (2009).
5. A. S. Rivkin, E. L. Volquardsen, B. E. Clark, The surface composition of Ceres: Discovery of carbonates and iron-rich clays. *Icarus* **185**, 563–567 (2006).
6. M. C. De Sanctis, E. Ammannito, A. Raponi, S. Marchi, T. B. McCord, H. Y. McSween, F. Capaccioni, M. T. Capria, F. G. Carrozzo, M. Ciarniello, A. Longobardo, F. Tosi, S. Fonte, M. Formisano, A. Frigeri, M. Giardino, G. Magni, E. Palomba, D. Turrini, F. Zambon, J.-P. Combe, W. Feldman, R. Jaumann, L. A. McFadden, C. M. Pieters, T. Prettyman, M. Toplis, C. A. Raymond, C. T. Russell, Ammoniated phyllosilicates with a likely outer Solar System origin on (1) Ceres. *Nature* **528**, 241–244 (2015).
7. D. Takir, J. P. Emery, H. Y. McSween, C. A. Hibbits, R. N. Clark, N. Pearson, A. Wang, Nature and degree of aqueous alteration in CM and CI carbonaceous chondrites. *Meteorit. Planet. Sci.* **48**, 1618–1637 (2013).
8. E. Ammannito, M. C. DeSanctis, M. Ciarniello, A. Frigeri, F. G. Carrozzo, J.-Ph. Combe, B. L. Ehlmann, S. Marchi, H. Y. McSween, A. Raponi, M. J. Toplis, F. Tosi, J. C. Castillo-Rogez, F. Capaccioni, M. T. Capria, S. Fonte, M. Giardino, R. Jaumann, A. Longobardo, S. P. Joy, G. Magni, T. B. McCord, L. A. McFadden, E. Palomba, C. M. Pieters, C. A. Polanskey, M. D. Rayman, C. A. Raymond, P. M. Schenk, F. Zambon, C. T. Russell, Distribution of phyllosilicates on the surface of Ceres. *Science* **353**, aaf4279 (2016).
9. M. C. De Sanctis, A. Raponi, E. Ammannito, M. Ciarniello, M. J. Toplis, H. Y. McSween, J. C. Castillo-Rogez, B. L. Ehlmann, F. G. Carrozzo, S. Marchi, F. Tosi, F. Zambon, F. Capaccioni, M. T. Capria, S. Fonte, M. Formisano, A. Frigeri, M. Giardino, A. Longobardo, G. Magni, E. Palomba, L. A. McFadden, C. M. Pieters, R. Jaumann, P. Schenk, R. Mugnuolo, C. A. Raymond, C. T. Russell, Bright carbonate deposits as evidence of aqueous alteration on (1) Ceres. *Nature* **536**, 54–57 (2016).
10. H. Y. McSween, J. P. Emery, A. S. Rivkin, M. J. Toplis, J. C. Castillo-Rogez, T. H. Prettyman, M. C. De Sanctis, C. M. Pieters, C. A. Raymond, C. T. Russell, Carbonaceous chondrites as analogs for the composition and alteration of Ceres. *Meteorit. Planet. Sci.* 1–12 (2017); http://dx.doi.org/10.1111/maps.12947.
11. C.K. Huang, P. F. Kerr, Infrared study of the carbonate mineral. *Am. Mineral.* **45**, 311–324 (1960).
12. M. C. De Sanctis, A. Coradini, E. Ammannito, G. Filacchione, M. T. Capria, S. Fonte, G. Magni, A. Barbis, A. Bini, M. Dami, I. Ficai-Veltroni, G. Preti; VIR Team, The VIR spectrometer. *Space Sci. Rev.* **163**, 329–369 (2011).
13. M. C. De Sanctis, E. Ammannito, H. Y. McSween, A. Raponi, S. Marchi, F. Capaccioni, M. T. Capria, F. G. Carrozzo, M. Ciarniello, S. Fonte, M. Formisano, A. Frigeri, M. Giardino, A. Longobardo, G. Magni, L. A. McFadden, E. Palomba, C. M. Pieters, F. Tosi, F. Zambon, C. A. Raymond, C. T. Russell, Localized aliphatic organic material on the surface of Ceres. *Science* **355**, 719–722 (2017).
14. E. Palomba, A. Longobardo, M. C. De Sanctis, N. T. Stein, B. Ehlmann, A. Raponi, M. Ciarniello, E. Ammannito, E. Cloutis, A. Galiano, F. G. Carrozzo, M. T. Capria, F. Zambon, F. Tosi, C. A. Raymond, C. T. Russell, Dawn/VIR Team, "Bright spots on Ceres: Occator, Oxo, and the others," 48th Lunar and Planetary Science Conference, abstract #1566 (2017).
15. F. Zambon, A. Raponi, F. Tosi, M. C. De Sanctis, L. A. McFadden, F. G. Carrozzo, A. Longobardo, M. Ciarniello, K. Krohn, K. Stephan, E. Palomba, C. M. Pieters, E. Ammannito, C. T. Russell, C. A. Raymond, Spectral analysis of Ahuna Mons from Dawn mission's visible-infrared spectrometer. *Geophys. Res. Lett.* **44**, 97–104 (2017).
16. K. Stephan, R. Jaumann, K. Krohn, N. Schmedemann, F. Zambon, F. Tosi, F. G. Carrozzo, L. A. McFadden, K. Otto, M. C. De Sanctis, E. Ammannito, K.-D. Matz, T. Roatsch, F. Preusker, C. A. Raymond, C. T. Russell, An investigation of the bluish material on Ceres. *Geophys. Res. Lett.* **44**, 1660–1668 (2017).
17. F. G. Carrozzo, M. C. De Sanctis, A. Raponi, E. Ammannito, J. Castillo-Rogez, B. L. Ehlmann, S. Marchi, N. Stein, M. Ciarniello, F. Tosi, F. Capaccioni, M. T. Capria, S. Fonte, M. Formisano, A. Frigeri, M. Giardino, A. Longobardo, G. Magni, E. Palomba, F. Zambon, C. A. Raymond, C. T. Russell, "Distribution of carbonates on genes," 49th Lunar and Planetary Science Conference, abstract #2336 (2018).
18. J.-P. Combe, T. B. McCord, F. Tosi, E. Ammannito, F. G. Carrozzo, M. C. De Sanctis, A. Raponi, S. Byrne, M. E. Landis, K. H. G. Hughson, C. A. Raymond, C. T. Russell, Detection of local H_2O exposed at the surface of Ceres. *Science* **353**, aaf3010 (2016).
19. M. C. De Sanctis, E. Ammannito, F. G. Carrozzo, J.-P. Combe, A. Raponi, M. Ciarniello, F. Tosi, C. Pieters, F. Zambon, A. Frigeri, C. Raymond, C. T. Russel, "Mineralogical analysis of the quadrangles AC-11 Sintana and AC-12 Toharu on the dwarf planet Ceres," *GSA Annual Meeting*, Denver, abstract #166-10 (2016).
20. M. Y. Zolotov, Formation of brucite and cronstedtite-bearing mineral assemblages on Ceres. *Icarus* **228**, 13–26 (2014).
21. J. C. Castillo-Rogez, T. B. McCord, Ceres' evolution and present state constrained by shape data. *Icarus* **205**, 443–459 (2010).
22. T. J. Bowling, F. J. Ciesla, S. Marchi, T. M. Davison, J. C. Castillo-Rogez, "Impact induced heating of occator crater on asteroid 1 Ceres," 47th Lunar and Planetary Science Conference, abstract #2268 (2016).
23. M. Y. Zolotov, Aqueous fluid composition in CI chondritic materials: Chemical equilibrium assessments in closed systems. *Icarus* **220**, 713–729 (2012).
24. F. Postberg, S. Kempf, J. Schmidt, N. Brilliantov, A. Beinsen, B. Abel, U. Buck, R. Srama, Sodium salts in E-ring ice grains from an ocean below the surface of Enceladus. *Nature* **459**, 1098–1101 (2009).
25. M. Y. Zolotov, E. L. Shock, Composition and stability of salts on the surface of Europa and their oceanic origin. *J. Geophys. Res.* **106**, 32815–32827 (2001).
26. T. H. Vu, R. Hodyss, P. V. Johnson, M. Choukroun, Preferential formation of sodium salts from frozen sodium-ammonium-chloride-carbonate brines – Implications for Ceres' bright spots. *Planet. Space Sci.* **141**, 73–77 (2017).
27. M.-Y. Zolotov, Aqueous origins of bright salt deposits on Ceres. *Icarus* **296**, 289–304 (2017).
28. N. Stein, B. Ehlmann, E. Ammannito, E. Palomba, M. C. De Sanctis, R. Jaumann, A. Nathues, C. A. Raymond, H. Hiesinger, P. Schenk, A. Longobardo, "Characteristics, formation, and evolution of Faculae (bright spots) on Ceres," 48th Lunar and Planetary Science Conference, abstract #2547 (2018).
29. D. L. Buczkowski, H. G. Sizemore, M. T. Bland, J. E. C. Scully, L. C. Quick, K. H. G. Hughson, L. M. Jozwiak, R. Park, F. Preusker, R. Jaumann, C. A. Raymond, C. T. Russell,

"Floor-fractured craters on Ceres: A geomorphic study and analysis of potential formation mechanisms," 49th Lunar and Planetary Science Conference, abstract #1614 (2018).
30. M. T. Bland, C. A. Raymond, P. M. Schenk, R. R. Fu, T. Kneissl, J. H. Pasckert, H. Hiesinger, F. Preusker, R. S. Park, S. Marchi, S. D. King, J. C. Castillo-Rogez, C. T. Russell, Composition and structure of the shallow subsurface of Ceres revealed by crater morphology. *Nat. Geosci.* **9**, 538–542 (2016).
31. R. Fu, A. I. Ermakov, S. Marchi, J. C. Castillo-Rogez, C. A. Raymond, B. H. Hager, M. T. Zuber, S. D. King, M. T. Bland, M. C. De Sanctis, F. Preusker, R. S. Park, C. T. Russell, The interior structure of Ceres as revealed by surface topography. *Earth Planet. Sci. Lett.* **476**, 153–164 (2017).
32. M. Neveu, S. J. Desch, Geochemistry, thermal evolution, and cryovolcanism on Ceres with a muddy ice mantle. *Geophys. Res. Lett.* **42**, 10197–10206 (2015).
33. O. Ruesch, T. Platz, P. Schenk, L. A. McFadden, J. C. Castillo-Rogez, L. C. Quick, S. Byrne, F. Preusker, D. P. O'Brien, N. Schmedemann, D. A. Williams, J.-Y. Li, M. T. Bland, H. Hiesinger, T. Kneissl, A. Neesemann, M. Schaefer, J. H. Pasckert, B. E. Schmidt, D. L. Buczkowski, M. V. Sykes, A. Nathues, T. Roatsch, M. Hoffmann, C. A. Raymond, C. T. Russell, Cryovolcanism on Ceres. *Science* **353**, aaf4286 (2016).
34. L. C. Quick, D. L. Buczkowski, J. E. C. Scully, O. Ruesch, J. Castillo-Rogez, C. A. Raymond, P. M. Schenk, H. G. Sizemore, M. V. Sykes, "Thermal and compositional evolution of a brine reservoir beneath Ceres' Occator crater: Implications for cryovolcanism at the surface," 49th Lunar and Planetary Science Conference, abstract #2921 (2018).
35. N. Schmedemann, T. Kneissl, A. Neesemann, K. Stephan, R. Jaumann, K. Krohn, G. G. Michael, K. D. Matz, K. A. Otto, C. A. Raymond, C. T. Russell, Timing of optical maturation of recently exposed material on Ceres. *Geophys. Res. Lett.* **43**, 11,987–11,993 (2016).
36. B. Hapke, *Theory of Reflectance and Emittance Spectroscopy* (Cambridge Univ. Press, 2012).
37. C. Carli, M. Ciarniello, F. Capaccioni, G. Serventi, M. Sgavetti, Spectral variability of plagioclase–mafic mixtures (2): Investigation of the optical constant and retrieved mineral abundance dependence on particle size distribution. *Icarus* **235**, 207–219 (2014).
38. A. Raponi, M. Ciarniello, F. Capaccioni, G. Filacchione, F. Tosi, M. C. De Sanctis, M. T. Capria, M. A. Barucci, A. Longobardo, E. Palomba, D. Kappel, G. Arnold, S. Mottola, B. Rousseau, E. Quirico, G. Rinaldi, S. Erard, D. Bockelee-Morvan, C. Leyrat, The temporal evolution of exposed water ice-rich areas on the surface of 67P/Churyumov–Gerasimenko: Spectral analysis. *MNRAS* **462**, S476–S490 (2016).
39. M. Ciarniello, M. C. De Sanctis, E. Ammannito, A. Raponi, A. Longobardo, E. Palomba, F. G. Carrozzo, F. Tosi, J.-Y. Li, S. E. Schröder, F. Zambon, A. Frigeri, S. Fonte, M. Giardino, C. M. Pieters, C. A. Raymond, C. T. Russell, Spectrophotometric properties of dwarf planet Ceres from the VIR spectrometer on board the Dawn mission. *Astron. Astrophys.* **598**, A130 (2017).
40. J. R. Davidsson, P. J. Gutiérrez, H. Rickman, Physical properties of morphological units on Comet 9P/Tempel 1 derived from near-IR Deep Impact spectra. *Icarus* **201**, 335–357 (2009).
41. F. G. Carrozzo, A. Raponi, M. C. De Sanctis, E. Ammannito, M. Giardino, E. D'Aversa, S. Fonte, F. Tosi, Artifacts reduction in VIR/Dawn data. *Rev. Sci. Instrum.* **87**, 124501 (2016).

Acknowledgments: We thank the Italian Space Agency (ASI) and NASA for supporting this work. The VIR instrument was funded and coordinated by the ASI and built by Selex ES, with the scientific leadership of the Institute for Space Astrophysics and Planetology, Italian National Institute for Astrophysics, and it is operated by the Institute for Space Astrophysics and Planetology (Rome, Italy). A portion of this work was carried out at the Jet Propulsion Laboratory, California Institute of Technology (USA) under contract to NASA.
Author contributions: F.G.C. wrote the manuscript, calibrated the data, and contributed to data analysis and interpretation. M.C.D.S. wrote the manuscript, coordinated the contributions and interpretation, and performed the analysis of the data. A.R. performed the spectral fits. E.A. calibrated the data and contributed to the data analysis. J.C.-R., B.L.E., S.M., and N.S. contributed to the spectral interpretation of the data and in writing the manuscript. M.C. provided optical constants from reflectance spectra. All authors helped with manuscript preparation. **Competing interests:** The authors declare that they have no competing interests. **Data and materials availability:** All data needed to evaluate the conclusions in the paper are present in the paper and/or the Supplementary Materials. Additional data related to this paper may be requested from the authors. Dawn data are archived in NASA's Planetary Data System. VIR spectral data may be obtained at http://sbn.psi.edu/pds/resource/dwncvir.html.

Submitted 17 May 2017
Accepted 23 January 2018
Published 14 March 2018
10.1126/sciadv.1701645

Citation: F. G. Carrozzo, M. C. De Sanctis, A. Raponi, E. Ammannito, J. Castillo-Rogez, B. L. Ehlmann, S. Marchi, N. Stein, M. Ciarniello, F. Tosi, F. Capaccioni, M. T. Capria, S. Fonte, M. Formisano, A. Frigeri, M. Giardino, A. Longobardo, G. Magni, E. Palomba, F. Zambon, C. A. Raymond, C. T. Russell, Nature, formation, and distribution of carbonates on Ceres. *Sci. Adv.* **4**, e1701645 (2018).